

STABILIZED MIXED APPROXIMATION OF AXISYMMETRIC BRINKMAN FLOWS^{*,**}

VERÓNICA ANAYA¹, DAVID MORA², CARLOS REALES³ AND RICARDO RUIZ-BAIER⁴

Abstract. This paper is devoted to the numerical analysis of an augmented finite element approximation of the axisymmetric Brinkman equations. Stabilization of the variational formulation is achieved by adding suitable Galerkin least-squares terms, allowing us to transform the original problem into a formulation better suited for performing its stability analysis. The sought quantities (here velocity, vorticity, and pressure) are approximated by Raviart–Thomas elements of arbitrary order $k \geq 0$, piecewise continuous polynomials of degree $k + 1$, and piecewise polynomials of degree k , respectively. The well-posedness of the resulting continuous and discrete variational problems is rigorously derived by virtue of the classical Babuška–Brezzi theory. We further establish *a priori* error estimates in the natural norms, and we provide a few numerical tests illustrating the behavior of the proposed augmented scheme and confirming our theoretical findings regarding optimal convergence of the approximate solutions.

Mathematics Subject Classification. 65N30, 65N12, 76D07, 65N15, 65J20.

Received July 22, 2014. Revised January 29, 2015.
Published online April 16, 2015.

1. INTRODUCTION

Cylindrical symmetry of both the data and the domain very often allows transforming an initially three-dimensional flow problem into a two-dimensional one, typically implying a substantial reduction in computational complexity. Apart from the advantages of considering an intrinsically axisymmetric problem in its natural configuration, such a reduction is particularly appealing in case of mixed approximations where additional

Keywords and phrases. Brinkman equations, axisymmetric domains, augmented mixed finite elements, well-posedness analysis, error estimates.

* *Dedicated to Rodolfo Rodríguez on his 60th birthday.*

** *This work has been supported by CONICYT-Chile through: FONDECYT postdoctorado project No. 3120197, project Inserción de Capital Humano Avanzado en la Academia No. 79112012, FONDECYT regular project No. 1140791, and project Anillo ANANUM-ACT1118; by DIUBB through project 120808 GI/EF, and by the Swiss National Science Foundation through the research grant PP00P2_144922.*

¹ GIMNAP, Departamento de Matemática, Facultad de Ciencias, Universidad del Bío-Bío, Casilla 5-C, Concepción, Chile. vanaya@ubiobio.cl

² GIMNAP, Departamento de Matemática, Facultad de Ciencias, Universidad del Bío-Bío, Casilla 5-C, Concepción, Chile, and Centro de Investigación en Ingeniería Matemática (CI²MA), Universidad de Concepción, Concepción, Chile. dmora@ubiobio.cl

³ Departamento de Matemáticas y Estadísticas, Universidad de Córdoba, Colombia. creales@correo.unicordoba.edu.co

⁴ Institute of Earth Sciences, UNIL-Mouline Géopolis, University of Lausanne, 1015 Lausanne, Switzerland. ricardo.ruizbaier@unil.ch

unknowns are introduced in order to accurately recover other fields of physical interest. The attached difficulty usually resides in the analysis and derivation of proper schemes to discretize axisymmetric formulations, due to the presence of singularities associated to weighted functional spaces and their respective finite dimensional counterparts, which can eventually translate into numerical singularity near the rotation axis (considered as $(r = 0, z)$), since a factor of $1/r$ appears in all volume integrals.

The main purpose here is to propose and analyze an augmented mixed finite element method for the accurate discretization of the axisymmetric Brinkman problem in its vorticity-velocity-pressure formulation. This system stands as a prototype model for the study of Stokes and Darcy flow regimes (see *e.g.* [43]), and it can also be employed to study semi-discretizations of transient Stokes equations. The vorticity (which is a scalar field in the axisymmetric case) is a sought quantity of key importance in *e.g.* subsurface flow, blood flow, and other applications where the patterns of rotational flow are of interest [42, 44], and it can be directly obtained from the present formulation, without resorting to numerical postprocessing (typically prone to accuracy loss unless high order methods are employed). Moreover, for external flows vorticity boundary data are more natural than *e.g.* pressure conditions, and velocity-vorticity formulations are more advantageous in problems defined in non-inertial frames of reference [46]. Also, in many regimes the vorticity gives much clearer insight about flow instabilities and it is typically concentrated in a specific region of the domain, where enough accuracy is mandatory. Augmentation of the variational formulation with penalized residual-based terms, usually allows to recast the saddle point problem as a strongly elliptic system, and it also provides a way of bypassing the so-called kernel property, or to yield inf-sup stable continuous and discrete formulations (see for instance, [27]). Our choice for the discretization of the governing equations consists in Raviart–Thomas elements of order k for the velocity field, piecewise continuous polynomials of degree $k + 1$ for the vorticity, and piecewise discontinuous polynomials of degree k for the pressure field, for $k \geq 0$.

1.1. Related work and specifics of this contribution

There exist several references dealing with the mathematical and numerical analysis of axisymmetric problems. For instance, the strategy of reducing the spatial dimension in finite element methods was applied to the axisymmetric Laplace problem in the early work [41]. Later on, numerous studies have been dedicated to different axisymmetric formulations of the Stokes equations employing finite differences [32, 39], and spectral, Mortar, Taylor–Hood, and stabilized finite elements (see [7, 10, 13, 14, 17, 22, 37, 38, 45]). Raviart–Thomas and Brezzi–Douglas–Marini mixed approximations for axisymmetric Darcy, and Stokes–Darcy flows were analyzed in [25, 26] using a generalization of the so-called Stenberg criterion. Recent contributions focusing on the design of numerical methods for axisymmetric formulations of coupled flow and transport problems can be found in *e.g.* [3, 20, 21, 33]. On the other hand, time-dependent and static Maxwell equations in axisymmetric singular domains were studied in [8, 9] by introducing a method based on a splitting of the space of solutions into a regular subspace and a singular one. In [36], a method was introduced to solve a time-harmonic Maxwell equation in axisymmetric domains using a Fourier decomposition. Such a technique was also employed in [41] for the axisymmetric Laplace equation. The development of multigrid schemes and rigorous estimates in weighted spaces was carried out in [24] for related problems. More recently, transient axisymmetric formulations with more general Ohm’s laws including velocity terms and being relevant in some industrial applications have been studied in [15, 16].

Up to our knowledge, the numerical analysis of finite element approximations of the generalized Stokes (or Brinkman) problem for the axisymmetric case has not been carried out yet. Nevertheless, in the Cartesian setting, there exist several methods including fully mixed, augmented, and stabilized formulations [11, 12, 29], also incorporating robust estimates with respect to viscosity [34, 40], whereas only a few recent contributions include formulations in terms of velocity, vorticity and pressure [5, 6, 48].

In this regard, we stress that the present study represents an extension to the vorticity-based Stokes problem analyzed in [4] in the sense that here we include the zeroth-order velocity component and introduce an axisymmetric formulation. On the other hand, the vorticity-based formulations for Brinkman equations analyzed in [5, 6, 48] are restricted to Cartesian two-dimensional domains, and therefore many practical applications

remain out of reach. An axisymmetric flow model was derived from a three-dimensional scenario in [1, 2], where the proposed numerical method was based on spectral finite elements. Here we have chosen a different discretization that retains optimal accuracy in complex domains and in the presence of coefficients with high gradients, and which requires reasonable regularity assumptions for the exact solutions and the data.

Our analysis of existence and uniqueness of solution to the continuous axisymmetric problem is carried out by introducing an augmented formulation that arises from including penalized least-squares terms to the original variational formulation. We point out that this step is not necessary in the continuous case, but (as we will address in full detail) the presence of the term $1/r$ in the volume integrals requires some sort of stabilizing terms in the discrete formulation that would further allow us to relax constraints related to *e.g.* discrete inf-sup conditions. Thus, we opt for augmenting both continuous and discrete problems so that the same arguments can be applied for their solvability analysis. The tools employed to establish the convergence of our scheme consist in a Céa estimate combined with properties of the global Raviart–Thomas and Lagrange interpolation operators.

1.2. Outline

We have structured the contents of this paper as follows. The remainder of this Section introduces the classical Brinkman problem in Cartesian coordinates, along with its reduction to the axisymmetric case. We also present a mixed formulation for this problem, and summarize some preliminary results needed for its analysis. Section 2, is devoted to the statement of a least-squares-based augmented formulation to the axisymmetric generalized Stokes problem, and we perform the solvability analysis employing standard arguments from the Babuška–Brezzi theory. The mixed finite element formulation is presented in Section 3, where we also rigorously derive the stability analysis and optimal error estimates. We continue with a few illustrative numerical examples collected in Section 4, which confirm the robustness and expected convergence properties of the proposed stabilized method, and we finally summarize the main aspects of this contribution in Section 5.

1.3. Linear Brinkman equations in Cartesian coordinates

The linear Brinkman equations governing the motion of an incompressible fluid can be written as the following boundary value problem:

$$\check{\sigma}\check{\mathbf{u}} - \nu\Delta\check{\mathbf{u}} + \nabla\check{p} = \check{\mathbf{f}} \quad \text{in } \check{\Omega}, \tag{1.1a}$$

$$\operatorname{div}\check{\mathbf{u}} = 0 \quad \text{in } \check{\Omega}, \tag{1.1b}$$

$$\check{\mathbf{u}} \cdot \check{\mathbf{n}} = 0 \quad \text{on } \partial\check{\Omega}, \tag{1.1c}$$

$$\operatorname{curl}\check{\mathbf{u}} \wedge \check{\mathbf{n}} = 0 \quad \text{on } \partial\check{\Omega}, \tag{1.1d}$$

where $\check{\Omega} \subset \mathbb{R}^3$ is a given spatial domain. In this formulation, the sought quantities are the local volume-average velocity $\check{\mathbf{u}}$ and the pressure field \check{p} . The positive model coefficients are the inverse permeability field $\check{\sigma} \in L^\infty(\check{\Omega})$, with $0 < \check{\sigma}_{\min} \leq \check{\sigma}(x, y, z) \leq \check{\sigma}_{\max}$ a.e. in $\check{\Omega}$, and the fluid viscosity $\nu > 0$. For constant permeability, the above system is also known as the generalized Stokes equations, and it allows in particular, to study spatial properties of the solutions to the time-dependent Stokes problem. In fact, the transient Stokes equations read

$$\begin{aligned} \partial_t\check{\mathbf{u}} - \frac{1}{\operatorname{Re}}\Delta\check{\mathbf{u}} + \nabla\check{p} &= \check{\mathbf{f}} \quad \text{in } \check{\Omega}, \\ \operatorname{div}\check{\mathbf{u}} &= 0 \quad \text{in } \check{\Omega}, \end{aligned} \tag{1.2}$$

which, after applying a backward Euler time discretization of the acceleration term, yield to the following system

$$\begin{aligned} \frac{1}{\Delta t}\check{\mathbf{u}}^{n+1} - \frac{1}{\operatorname{Re}}\Delta\check{\mathbf{u}}^{n+1} + \nabla\check{p}^{n+1} &= \check{\mathbf{f}}^{n+1} + \frac{1}{\Delta t}\check{\mathbf{u}}^n \quad \text{in } \check{\Omega}, \\ \operatorname{div}\check{\mathbf{u}}^{n+1} &= 0 \quad \text{in } \check{\Omega}. \end{aligned} \tag{1.3}$$

That is, the solution of (1.2) requires to solve (1.3) at each time step.

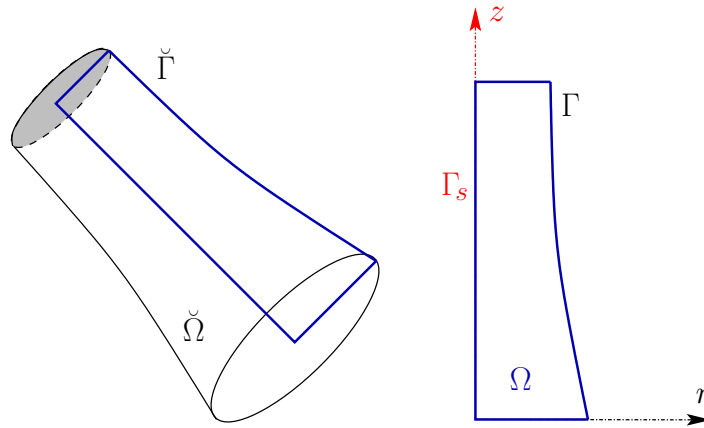


FIGURE 1. Sketch of a full three dimensional domain $\check{\Omega}$ with boundary $\check{\Gamma}$ and the axisymmetric meridional domain Ω with boundary Γ (left and right, respectively). Here Γ_s stands for the symmetry axis.

When the forcing term and the inverse permeability are axisymmetric, they can be replaced by \mathbf{f} and σ , respectively, with $0 < \sigma_{\min} \leq \sigma(r, z) \leq \sigma_{\max}$ a.e. in Ω , and system (1.1a)–(1.1d) can be recast as two uncoupled problems in the so-called meridional domain Ω (see Fig. 1): a problem involving only the unknown u_θ , and a problem with unknowns u_r, u_z and p . Here, we focus on the second case.

1.4. Preliminaries and axisymmetric formulation

In this section, we define appropriate weighted Sobolev spaces that will be used in the sequel and establish some of their properties; the corresponding proofs can be found in [13, 31, 41] (see also [24, 30, 35] for further general results on weighted Sobolev spaces, and some applications, respectively).

For an integer $\ell \geq 0$ and a real $1 \leq q \leq \infty$, $L^q(\Omega)$ is the set of measurable functions φ such that $(\int_\Omega \varphi^q dx)^{1/q} < \infty$ and $W^{\ell, q}(\Omega)$ denotes the usual Sobolev space of functions whose derivatives up to order ℓ are in $L^q(\Omega)$. Unless otherwise specified, we denote vector variables and spaces in bold.

In general, we will denote with $\check{\cdot}$ a quantity associated to the three-dimensional domain $\check{\Omega}$, whereas vector fields associated to the axisymmetric restriction will be denoted by $\mathbf{v} = (v_r, v_z)$. Let us also recall that the axisymmetric counterparts of the usual differential operators acting on vectors and scalars read

$$\begin{aligned} \operatorname{div}_a \mathbf{v} &:= \partial_z v_z + \frac{1}{r} \partial_r (r v_r) = \partial_r v_r + r^{-1} v_r + \partial_z v_z, & \operatorname{rot} \mathbf{v} &:= \partial_r v_z - \partial_z v_r, \\ \nabla \varphi &:= (\partial_r \varphi, \partial_z \varphi)^T, & \operatorname{curl}_a \varphi &:= (\partial_z \varphi, -r^{-1} \partial_r (r \varphi))^T. \end{aligned}$$

After introducing the (scaled) vorticity field $\omega = \sqrt{\nu} \operatorname{rot} \mathbf{u}$, we notice that system (1.1a)–(1.1d) is equivalent to

$$\sigma \mathbf{u} + \sqrt{\nu} \operatorname{curl}_a \omega + \nabla p = \mathbf{f} \quad \text{in } \Omega, \tag{1.4a}$$

$$\omega - \sqrt{\nu} \operatorname{rot} \mathbf{u} = 0 \quad \text{in } \Omega, \tag{1.4b}$$

$$\operatorname{div}_a \mathbf{u} = 0 \quad \text{in } \Omega, \tag{1.4c}$$

$$\mathbf{u} \cdot \mathbf{n} = 0 \quad \text{on } \Gamma, \tag{1.4d}$$

$$\omega = 0 \quad \text{on } \Gamma. \tag{1.4e}$$

At times, we will need appropriate weighted Sobolev spaces which we introduce in what follows, along with some of their main properties; the corresponding proofs and further general results about weighted Sobolev spaces can be found in *e.g.* [13, 35, 41]. To alleviate the notation, we will denote the partial derivatives by ∂_r and ∂_z .

Let $L^p_\alpha(\Omega)$ denote the weighted Lebesgue space of all measurable functions φ defined in Ω for which

$$\|\varphi\|_{L^p_\alpha(\Omega)} := \int_\Omega |\varphi|^p r^\alpha \, dr dz < \infty.$$

The subspace $L^2_{1,0}(\Omega)$ of $L^2_1(\Omega)$ contains functions q with zero weighted integral:

$$\int_\Omega qr \, dr dz = 0.$$

The weighted Sobolev space $H^k_r(\Omega)$ consists of all functions in $L^2_1(\Omega)$ whose derivatives up to order k are also in $L^2_1(\Omega)$. This space is provided with norms and semi-norms defined in the standard way; in particular,

$$|\varphi|_{H^1_1(\Omega)}^2 := \int_\Omega \left(|\partial_r \varphi|^2 + |\partial_z \varphi|^2 \right) r \, dr dz,$$

and $\tilde{H}^1_1(\Omega) := H^1_1(\Omega) \cap L^2_{-1}(\Omega)$ endowed with the following ν -dependent norm

$$\|\varphi\|_{\tilde{H}^1_1(\Omega)} := \left(\|\varphi\|_{L^2_1(\Omega)}^2 + \nu |\varphi|_{H^1_1(\Omega)}^2 + \nu \|\varphi\|_{L^2_{-1}(\Omega)}^2 \right)^{1/2},$$

is a Hilbert space. We will also require the following weighted scalar and vectorial functional spaces:

$$\begin{aligned} H^1_{1,\diamond}(\Omega) &:= \{ \varphi \in H^1_1(\Omega); \varphi = 0 \text{ on } \Gamma \}, & \tilde{H}^1_{1,\diamond}(\Omega) &:= \{ \varphi \in \tilde{H}^1_1(\Omega); \varphi = 0 \text{ on } \Gamma \}, \\ \mathbf{H}(\text{div}_a, \Omega) &:= \{ \mathbf{v} \in L^2_1(\Omega)^2; \text{div}_a \mathbf{v} \in L^2_1(\Omega) \}, & \mathbf{H}_0(\text{div}_a, \Omega) &:= \{ \mathbf{v} \in L^2_1(\Omega)^2; \text{div}_a \mathbf{v} = 0 \text{ in } \Omega \}, \\ \mathbf{H}_\diamond(\text{div}_a, \Omega) &:= \{ \mathbf{v} \in \mathbf{H}(\text{div}_a, \Omega); \mathbf{v} \cdot \mathbf{n} = 0 \text{ on } \Gamma \}, & \mathbf{H}(\mathbf{curl}_a, \Omega) &:= \{ \varphi \in L^2_1(\Omega); \mathbf{curl}_a \varphi \in L^2_1(\Omega)^2 \}, \\ \mathbf{H}(\text{rot}, \Omega) &:= \{ \mathbf{v} \in L^2_1(\Omega)^2; \text{rot } \mathbf{v} \in L^2_1(\Omega) \}. \end{aligned}$$

The spaces $\mathbf{H}(\text{div}_a, \Omega)$ and $\mathbf{H}(\mathbf{curl}_a, \Omega)$ are endowed respectively by the norms:

$$\|\mathbf{v}\|_{\mathbf{H}(\text{div}_a, \Omega)} := \left(\|\mathbf{v}\|_{L^2_1(\Omega)^2}^2 + \|\text{div}_a \mathbf{v}\|_{L^2_1(\Omega)}^2 \right)^{1/2}, \quad \|\varphi\|_{\mathbf{H}(\mathbf{curl}_a, \Omega)} := \left(\|\varphi\|_{L^2_1(\Omega)}^2 + \nu \|\mathbf{curl}_a \varphi\|_{L^2_1(\Omega)^2}^2 \right)^{1/2}.$$

In addition, notice that the norms $\|\cdot\|_{\mathbf{H}(\mathbf{curl}_a, \Omega)}$ and $\|\cdot\|_{\tilde{H}^1_1(\Omega)}$ are equivalent, and for any $\varphi \in \tilde{H}^1_1(\Omega)$ they verify the following relations:

$$\sqrt{\nu} \|\mathbf{curl}_a \varphi\|_{L^2_1(\Omega)^2} \leq \sqrt{2} \|\varphi\|_{\tilde{H}^1_1(\Omega)}, \tag{1.5}$$

$$\|\varphi\|_{\tilde{H}^1_1(\Omega)} \leq \|\varphi\|_{\mathbf{H}(\mathbf{curl}_a, \Omega)} \leq \sqrt{2} \|\varphi\|_{\tilde{H}^1_1(\Omega)}. \tag{1.6}$$

We now collect some useful results to be employed in the sequel (see [2]).

Lemma 1.1. *Let $H^{1/2}_1(\Gamma)$ be the trace space of functions in $H^1_1(\Omega)$. The normal trace operator on Γ is defined by $\mathbf{v} \mapsto \mathbf{v} \cdot \mathbf{n}|_\Gamma$, and it is continuous from $\mathbf{H}(\text{div}_a, \Omega)$ into the dual space of $H^{1/2}_1(\Gamma)$.*

Lemma 1.2. *For any $\mathbf{v} \in \mathbf{H}(\text{div}_a, \Omega)$ and $q \in H^1_1(\Omega)$, the following Green formula holds*

$$\int_\Omega \text{div}_a \mathbf{v} q r \, dr dz + \int_\Omega \mathbf{v} \cdot \nabla q r \, dr dz = \int_\Gamma \mathbf{v} \cdot \mathbf{n} q \, ds.$$

Lemma 1.3. For any $\mathbf{v} \in \mathbf{H}(\text{rot}, \Omega)$ and $\varphi \in \tilde{\mathbf{H}}_1^1(\Omega)$, we have the following Green formula

$$\int_{\Omega} \mathbf{v} \cdot \mathbf{curl}_{\mathbf{a}} \varphi r \, dr dz - \int_{\Omega} \varphi \text{rot } \mathbf{v} r \, dr dz = \int_{\Gamma} \mathbf{v} \cdot \mathbf{t} \varphi \, ds.$$

Let us now test system (1.4a)–(1.4e) against functions $\mathbf{v} \in \mathbf{H}_{\circ}(\text{div}_{\mathbf{a}}, \Omega)$, $\varphi \in \tilde{\mathbf{H}}_{1,\diamond}^1(\Omega)$ and $q \in L_{1,0}^2(\Omega)$:

$$\begin{aligned} \int_{\Omega} \sigma \mathbf{u} \cdot \mathbf{v} r \, dr dz + \sqrt{\nu} \int_{\Omega} \mathbf{curl}_{\mathbf{a}} \omega \cdot \mathbf{v} r \, dr dz + \int_{\Omega} \nabla p \cdot \mathbf{v} r \, dr dz &= \int_{\Omega} \mathbf{f} \cdot \mathbf{v} r \, dr dz, \\ \int_{\Omega} \omega \varphi r \, dr dz - \sqrt{\nu} \int_{\Omega} \text{rot } \mathbf{u} \varphi r \, dr dz &= 0, \\ \int_{\Omega} \text{div}_{\mathbf{a}} \mathbf{u} q r \, dr dz &= 0. \end{aligned}$$

Combining Lemmas 1.2 and 1.3 with a direct application of the boundary conditions yields

$$\begin{aligned} \int_{\Omega} \sigma \mathbf{u} \cdot \mathbf{v} r \, dr dz + \sqrt{\nu} \int_{\Omega} \mathbf{curl}_{\mathbf{a}} \omega \cdot \mathbf{v} r \, dr dz - \int_{\Omega} \text{div}_{\mathbf{a}} \mathbf{v} p r \, dr dz &= \int_{\Omega} \mathbf{f} \cdot \mathbf{v} r \, dr dz, \\ \int_{\Omega} \omega \varphi r \, dr dz - \sqrt{\nu} \int_{\Omega} \mathbf{u} \cdot \mathbf{curl}_{\mathbf{a}} \varphi r \, dr dz &= 0, \\ \int_{\Omega} \text{div}_{\mathbf{a}} \mathbf{u} q r \, dr dz &= 0. \end{aligned}$$

This variational problem can be rewritten as follows: Find $(\mathbf{u}, \omega, p) \in \mathbf{H}_{\circ}(\text{div}_{\mathbf{a}}, \Omega) \times \tilde{\mathbf{H}}_{1,\diamond}^1(\Omega) \times L_{1,0}^2(\Omega)$ such that

$$\begin{aligned} a(\mathbf{u}, \mathbf{v}) + b(\mathbf{v}, \omega) + c(\mathbf{v}, p) &= F(\mathbf{v}) \quad \forall \mathbf{v} \in \mathbf{H}_{\circ}(\text{div}_{\mathbf{a}}, \Omega), \\ b(\mathbf{u}, \varphi) - d(\omega, \varphi) &= 0 \quad \forall \varphi \in \tilde{\mathbf{H}}_{1,\diamond}^1(\Omega), \\ c(\mathbf{u}, q) &= 0 \quad \forall q \in L_{1,0}^2(\Omega), \end{aligned} \tag{1.7}$$

where the involved bilinear forms and linear functionals are defined as follows

$$\begin{aligned} a(\mathbf{u}, \mathbf{v}) &:= \int_{\Omega} \sigma \mathbf{u} \cdot \mathbf{v} r \, dr dz, & b(\mathbf{v}, \omega) &:= \sqrt{\nu} \int_{\Omega} \mathbf{curl}_{\mathbf{a}} \omega \cdot \mathbf{v} r \, dr dz, \\ c(\mathbf{v}, p) &:= - \int_{\Omega} \text{div}_{\mathbf{a}} \mathbf{v} p r \, dr dz, & d(\omega, \varphi) &:= \int_{\Omega} \omega \varphi r \, dr dz, & F(\mathbf{v}) &:= \int_{\Omega} \mathbf{f} \cdot \mathbf{v} r \, dr dz. \end{aligned}$$

2. A STABILIZED MIXED FORMULATION FOR THE AXISYMMETRIC BRINKMAN PROBLEM

In this section, we introduce and analyze a mixed variational formulation of the problem. As we will address in full detail, an augmented dual-mixed variational formulation will permit us to analyze the problem directly under the classical Babuška–Brezzi theory [19, 27].

2.1. Problem statement and preliminary results

Our goal here is to introduce an augmented dual-mixed variational formulation of system (1.4a)–(1.4e), where our strategy is to enrich the mixed variational formulation (1.7) with a residual term arising from equations (1.4a) and (1.4c).

More precisely, we add to the variational problem (1.7) the following Galerkin least-squares terms:

$$\kappa_1 \sqrt{\nu} \int_{\Omega} (\sigma \mathbf{u} + \sqrt{\nu} \mathbf{curl}_{\mathbf{a}} \omega + \nabla p - \mathbf{f}) \cdot \mathbf{curl}_{\mathbf{a}} \varphi r \, dr dz = 0 \quad \forall \varphi \in \tilde{\mathbf{H}}_{1,\diamond}^1(\Omega), \tag{2.1}$$

$$\kappa_2 \int_{\Omega} \operatorname{div}_a \mathbf{u} \operatorname{div}_a \mathbf{v} r \, dr dz = 0 \quad \forall \mathbf{v} \in \mathbf{H}_\diamond(\operatorname{div}_a, \Omega), \tag{2.2}$$

where κ_1 and κ_2 are positive parameters to be specified later. From Lemma 1.3, the fact that $\operatorname{rot}(\nabla p) = 0$, and the boundary condition given in (1.4e), we may rewrite (2.1) equivalently as follows:

$$\kappa_1 \sqrt{\nu} \int_{\Omega} \sigma \mathbf{u} \cdot \operatorname{curl}_a \varphi r \, dr dz + \kappa_1 \nu \int_{\Omega} \operatorname{curl}_a \omega \cdot \operatorname{curl}_a \varphi r \, dr dz = \kappa_1 \sqrt{\nu} \int_{\Omega} \mathbf{f} \cdot \operatorname{curl}_a \varphi r \, dr dz,$$

for all $\varphi \in \tilde{\mathbf{H}}_{1,\diamond}^1(\Omega)$. In this way, and in addition to (1.7), we propose the following augmented variational formulation:

Find $((\mathbf{u}, \omega), p) \in (\mathbf{H}_\diamond(\operatorname{div}_a, \Omega) \times \tilde{\mathbf{H}}_{1,\diamond}^1(\Omega)) \times L_{1,0}^2(\Omega)$ such that

$$\begin{aligned} A((\mathbf{u}, \omega), (\mathbf{v}, \varphi)) + B((\mathbf{v}, \varphi), p) &= G(\mathbf{v}, \varphi) \quad \forall (\mathbf{v}, \varphi) \in \mathbf{H}_\diamond(\operatorname{div}_a, \Omega) \times \tilde{\mathbf{H}}_{1,\diamond}^1(\Omega), \\ B((\mathbf{u}, \omega), q) &= 0 \quad \forall q \in L_{1,0}^2(\Omega), \end{aligned} \tag{2.3}$$

where the bilinear forms and the linear functional are defined by

$$\begin{aligned} A((\mathbf{u}, \omega), (\mathbf{v}, \varphi)) &:= \int_{\Omega} \sigma \mathbf{u} \cdot \mathbf{v} r \, dr dz + \sqrt{\nu} \int_{\Omega} \operatorname{curl}_a \omega \cdot \mathbf{v} r \, dr dz - \sqrt{\nu} \int_{\Omega} \operatorname{curl}_a \varphi \cdot \mathbf{u} r \, dr dz \\ &\quad + \int_{\Omega} \omega \varphi r \, dr dz + \kappa_1 \sqrt{\nu} \int_{\Omega} \sigma \mathbf{u} \cdot \operatorname{curl}_a \varphi r \, dr dz \\ &\quad + \kappa_1 \nu \int_{\Omega} \operatorname{curl}_a \omega \cdot \operatorname{curl}_a \varphi r \, dr dz + \kappa_2 \int_{\Omega} \operatorname{div}_a \mathbf{u} \operatorname{div}_a \mathbf{v} r \, dr dz, \end{aligned} \tag{2.4}$$

$$B((\mathbf{v}, \varphi), q) := - \int_{\Omega} q \operatorname{div}_a \mathbf{v} r \, dr dz, \tag{2.5}$$

and

$$G(\mathbf{v}, \varphi) := \kappa_1 \sqrt{\nu} \int_{\Omega} \mathbf{f} \cdot \operatorname{curl}_a \varphi r \, dr dz + \int_{\Omega} \mathbf{f} \cdot \mathbf{v} r \, dr dz,$$

for all $(\mathbf{u}, \omega), (\mathbf{v}, \varphi) \in \mathbf{H}_\diamond(\operatorname{div}_a, \Omega) \times \tilde{\mathbf{H}}_{1,\diamond}^1(\Omega)$, and $q \in L_{1,0}^2(\Omega)$.

2.2. Unique solvability of the stabilized formulation

Next, we will prove that our stabilized variational formulation (2.3) satisfies the hypotheses of the Babuška–Brezzi theory, which yields the unique solvability and continuous dependence on the data of this variational formulation.

First, we observe that the bilinear forms A and B , and the linear functional G are bounded by a constant independent of ν . More precisely, there exist $C_1, C_2, C_3 > 0$ such that

$$\begin{aligned} |A((\mathbf{u}, \omega), (\mathbf{v}, \varphi))| &\leq C_1 \|(\mathbf{u}, \omega)\|_{\mathbf{H}(\operatorname{div}_a, \Omega) \times \tilde{\mathbf{H}}_1^1(\Omega)} \|(\mathbf{v}, \varphi)\|_{\mathbf{H}(\operatorname{div}_a, \Omega) \times \tilde{\mathbf{H}}_1^1(\Omega)}, \\ |B((\mathbf{v}, \varphi), q)| &\leq C_2 \|(\mathbf{v}, \varphi)\|_{\mathbf{H}(\operatorname{div}_a, \Omega) \times \tilde{\mathbf{H}}_1^1(\Omega)} \|q\|_{L_{1,0}^2(\Omega)}, \\ |G(\mathbf{v}, \varphi)| &\leq C_3 \|(\mathbf{v}, \varphi)\|_{\mathbf{H}(\operatorname{div}_a, \Omega) \times \tilde{\mathbf{H}}_1^1(\Omega)}. \end{aligned}$$

The following lemma shows that the bilinear form A is elliptic over the whole space $\mathbf{H}_\diamond(\operatorname{div}_a, \Omega) \times \tilde{\mathbf{H}}_{1,\diamond}^1(\Omega)$, provided that the stabilization parameters κ_1 and κ_2 are chosen adequately.

Lemma 2.1. *Suppose that $\kappa_1 \in (0, \frac{2}{\sigma_{\min}})$ and $\kappa_2 > 0$. Therefore, there exists $\alpha > 0$ independent of ν , such that*

$$A((\mathbf{v}, \varphi), (\mathbf{v}, \varphi)) \geq \alpha \|(\mathbf{v}, \varphi)\|_{\mathbf{H}(\operatorname{div}_a, \Omega) \times \tilde{\mathbf{H}}_1^1(\Omega)}^2 \quad \forall (\mathbf{v}, \varphi) \in \mathbf{H}_\diamond(\operatorname{div}_a, \Omega) \times \tilde{\mathbf{H}}_{1,\diamond}^1(\Omega).$$

Proof. Given $(\mathbf{v}, \varphi) \in \mathbf{H}_\circ(\operatorname{div}_a, \Omega) \times \tilde{\mathbf{H}}^1_{1,\phi}(\Omega)$, a combination of (2.4) with Cauchy–Schwarz inequality readily gives

$$\begin{aligned} A((\mathbf{v}, \varphi), (\mathbf{v}, \varphi)) &\geq \sigma_{\min} \|\mathbf{v}\|_{L^2_1(\Omega)^2}^2 + \|\varphi\|_{L^2_1(\Omega)}^2 + \kappa_1 \sqrt{\nu} \sigma_{\min} \int_{\Omega} \mathbf{v} \cdot \mathbf{curl}_a \varphi r \, dr dz \\ &\quad + \kappa_1 \nu \|\mathbf{curl}_a \varphi\|_{L^2_1(\Omega)^2}^2 + \kappa_2 \|\operatorname{div}_a \mathbf{v}\|_{L^2_1(\Omega)}^2, \\ &\geq \sigma_{\min} \|\mathbf{v}\|_{L^2_1(\Omega)^2}^2 + \|\varphi\|_{L^2_1(\Omega)}^2 - \kappa_1 \sqrt{\nu} \sigma_{\min} \|\mathbf{v}\|_{L^2_1(\Omega)^2} \|\mathbf{curl}_a \varphi\|_{L^2_1(\Omega)^2} \\ &\quad + \kappa_1 \nu \|\mathbf{curl}_a \varphi\|_{L^2_1(\Omega)^2}^2 + \kappa_2 \|\operatorname{div}_a \mathbf{v}\|_{L^2_1(\Omega)}^2, \\ &\geq \sigma_{\min} \|\mathbf{v}\|_{L^2_1(\Omega)^2}^2 + \|\varphi\|_{L^2_1(\Omega)}^2 - \frac{\sigma_{\min}}{2} \|\mathbf{v}\|_{L^2_1(\Omega)^2}^2 - \frac{\kappa_1^2 \nu \sigma_{\min}}{2} \|\mathbf{curl}_a \varphi\|_{L^2_1(\Omega)^2}^2 \\ &\quad + \kappa_1 \nu \|\mathbf{curl}_a \varphi\|_{L^2_1(\Omega)^2}^2 + \kappa_2 \|\operatorname{div}_a \mathbf{v}\|_{L^2_1(\Omega)}^2, \\ &= \frac{\sigma_{\min}}{2} \|\mathbf{v}\|_{L^2_1(\Omega)^2}^2 + \kappa_2 \|\operatorname{div}_a \mathbf{v}\|_{L^2_1(\Omega)}^2 + \|\varphi\|_{L^2_1(\Omega)}^2 \\ &\quad + \kappa_1 \left(1 - \frac{\kappa_1 \sigma_{\min}}{2}\right) \nu \|\mathbf{curl}_a \varphi\|_{L^2_1(\Omega)^2}^2, \\ &\geq \min\left\{\frac{\sigma_{\min}}{2}, \kappa_2\right\} \|\mathbf{v}\|_{\mathbf{H}(\operatorname{div}_a, \Omega)}^2 + \min\left\{1, \kappa_1 \left(1 - \frac{\kappa_1 \sigma_{\min}}{2}\right)\right\} \|\varphi\|_{\mathbf{H}(\mathbf{curl}_a, \Omega)}^2, \\ &\geq \alpha \|(\mathbf{v}, \varphi)\|_{\mathbf{H}(\operatorname{div}_a, \Omega) \times \tilde{\mathbf{H}}^1_1(\Omega)}^2, \end{aligned}$$

where we have also employed (1.6). We observe that the constant α in the above estimate is depending on $\kappa_1, \kappa_2, \sigma$, but not on the viscosity ν . The proof is then complete. \square

The following result establishes the corresponding inf-sup condition for the bilinear form B (see (2.5)). Its proof is a direct consequence of the three-dimensional corresponding inf-sup condition (see [18], Lem. IX.1). For more details we refer to *e.g.* ([2], Lem. 2.6).

Lemma 2.2. *There exists $\beta > 0$ independent of $\kappa_1, \kappa_2, \sigma$ and ν , such that the following holds*

$$\sup_{\substack{(\mathbf{v}, \varphi) \in \mathbf{H}_\circ(\operatorname{div}_a, \Omega) \times \tilde{\mathbf{H}}^1_{1,\phi}(\Omega) \\ (\mathbf{v}, \varphi) \neq 0}} \frac{|B((\mathbf{v}, \varphi), q)|}{\|(\mathbf{v}, \varphi)\|_{\mathbf{H}(\operatorname{div}_a, \Omega) \times \tilde{\mathbf{H}}^1_1(\Omega)}} \geq \beta \|q\|_{L^2_1(\Omega)} \quad \forall q \in L^2_{1,0}(\Omega).$$

We are now in a position to state the main result of this section which yields the solvability of the continuous formulation (2.3).

Theorem 2.3. *There exists a unique solution $((\mathbf{u}, \omega), p) \in (\mathbf{H}_\circ(\operatorname{div}_a, \Omega) \times \tilde{\mathbf{H}}^1_{1,\phi}(\Omega)) \times L^2_{1,0}(\Omega)$ to problem (2.3) and there exists a positive constant $C > 0$, independent of ν , such that the following continuous dependence result holds:*

$$\|((\mathbf{u}, \omega), p)\|_{(\mathbf{H}(\operatorname{div}_a, \Omega) \times \tilde{\mathbf{H}}^1_1(\Omega)) \times L^2_1(\Omega)} \leq C \|\mathbf{f}\|_{L^2_1(\Omega)^2}.$$

Proof. By virtue of Lemmas 2.1 and 2.2, the proof follows from a straightforward application of ([19], Thm. II.1.1). \square

3. MIXED FINITE ELEMENT APPROXIMATION

In this section, we construct a finite element scheme associated to (2.3), define explicit finite element subspaces yielding the unique solvability of the discrete scheme, derive the *a priori* error estimates, and provide the rate of convergence of the method.

3.1. Statement of the stabilized discrete scheme

Let $\{\mathcal{T}_h\}_{h>0}$ be a regular family of triangulations of Ω by triangles T with mesh size h . For $S \subset \bar{\Omega}$, we denote by $\mathbb{P}_k(S)$ and $\tilde{\mathbb{P}}_k(S)$, $k \in \mathbb{N} \cup \{0\}$, the set of polynomials of degree $\leq k$, and the set of homogeneous polynomials of degree k on S , respectively. We begin by introducing some notation and basic definitions presented in [25]. First, we recall the definition of the two-dimensional Raviart–Thomas spaces, next we focus on the axisymmetric case. Let \mathcal{E}_h be the set of all edges of the triangulation \mathcal{T}_h , and given $T \in \mathcal{T}_h$, let $\mathcal{E}(T)$ be the set of its edges, and we define the space

$$R_k(\partial T) := \{\phi \in L^2(\partial T) : \phi|_e \in \mathbb{P}_k(e), e \in \mathcal{E}(T)\}.$$

For $\Omega \subset \mathbb{R}^2$, $T \in \mathcal{T}_h$, let us denote by $\mathbf{RT}_k(T)$ the Raviart–Thomas space, which is defined by

$$\mathbf{RT}_k(T) := \mathbb{P}_k(T)^2 + \begin{bmatrix} r \\ z \end{bmatrix} \tilde{\mathbb{P}}_k(T),$$

where, for $\mathbf{v} \in \mathbf{RT}_k(T)$, \mathbf{n}_T the unit outer normal on ∂T , the degrees of freedom are given by

$$\int_{\mathcal{E}(T)} \mathbf{v} \cdot \mathbf{n}_T \phi \quad \forall \phi \in R_k(\partial T),$$

for $k \geq 0$, and

$$\int_T \mathbf{v} \cdot \boldsymbol{\phi} \quad \forall \boldsymbol{\phi} \in \mathbb{P}_{k-1}(T)^2,$$

for $k \geq 1$. Regarding the axisymmetric case, we define $\mathcal{E}^a(T)$ as the set of edges in the triangulation \mathcal{T}_h contained in T , but which do not lie along the symmetry axis Γ_s . Additionally, we introduce the set

$$\mathcal{E}^a(\mathcal{T}_h) := \cup_{T \in \mathcal{T}_h} \mathcal{E}^a(T),$$

and define

$$\begin{aligned} \mathbf{RT}_k^a(T) &:= \{\mathbf{v} \in \mathbf{RT}_k(T) : \mathbf{v} \cdot \mathbf{n}|_{\Gamma_s} = 0\} \\ &= \left\{ \begin{bmatrix} v_r \\ v_z \end{bmatrix} \in \mathbf{RT}_k(T) : v_r|_{\Gamma_s} = 0 \right\}, \end{aligned}$$

where the degrees of freedom (for $k \geq 0$) are given by

$$\int_{\mathcal{E}(T)} \mathbf{v} \cdot \mathbf{n}_T \phi r \, dr dz \quad \forall \phi \in R_k(\partial T),$$

and for $k \geq 1$, by

$$\int_T \mathbf{v} \cdot \boldsymbol{\phi} r \, dr dz \quad \forall \boldsymbol{\phi} \in \mathbb{P}_{k-1}(T)^2.$$

Let us now make precise the choice of finite element subspaces, for any $k \geq 0$:

$$\mathbf{H}_h := \{\mathbf{v}_h \in \mathbf{H}_\diamond(\text{div}_a, \Omega) : \mathbf{v}_h|_T \in \mathbf{RT}_k^a(T) \, \forall T \in \mathcal{T}_h\}, \tag{3.1}$$

$$\mathbf{Z}_h := \{\varphi_h \in \tilde{\mathbf{H}}_{1,\diamond}^1(\Omega) : \varphi_h|_T \in \mathbb{P}_{k+1}(T) \, \forall T \in \mathcal{T}_h\}, \tag{3.2}$$

$$\mathbf{Q}_h := \{q_h \in L_{1,0}^2(\Omega) : q_h|_T \in \mathbb{P}_k(T) \, \forall T \in \mathcal{T}_h\}. \tag{3.3}$$

Then, the Galerkin scheme associated with the continuous variational formulation (2.3) reads as follows:

Find $((\mathbf{u}_h, \omega_h), p_h) \in (\mathbf{H}_h \times \mathbf{Z}_h) \times \mathbf{Q}_h$ such that

$$\begin{aligned} A((\mathbf{u}_h, \omega_h), (\mathbf{v}_h, \varphi_h)) + B((\mathbf{v}_h, \varphi_h), p_h) &= G(\mathbf{v}_h, \varphi_h) \quad \forall (\mathbf{v}_h, \varphi_h) \in \mathbf{H}_h \times \mathbf{Z}_h, \\ B((\mathbf{u}_h, \omega_h), q_h) &= 0 \quad \forall q_h \in \mathbf{Q}_h. \end{aligned} \tag{3.4}$$

Remark 3.1. Notice that the well-posedness of the continuous variational formulation (1.7) can be readily established using, for instance, the recent results from [28] related to a generalization of the Babuška–Brezzi theory (see also our Thm. 2.3). However, the discrete problem (3.4) *does not lie in such a framework* since the axisymmetric divergence of any $\mathbf{v}_h \in \mathbf{H}_h$ does not belong to \mathbf{Q}_h .

3.2. Solvability and stability analysis of the discrete formulation

In view of Remark 3.1, we now devote ourselves to provide discrete counterparts of Lemmas 2.1 and 2.2, which will eventually conclude the solvability and stability of problem (3.4). With this aim, we first state the following result, which is a direct consequence of Lemma 2.1.

Lemma 3.2. *Assuming that $\kappa_1 \in (0, \frac{2}{\sigma_{\min}})$ and $\kappa_2 > 0$, then there exists $\alpha > 0$ independent of ν and h , such that*

$$A((\mathbf{v}_h, \varphi_h), (\mathbf{v}_h, \varphi_h)) \geq \alpha \|(\mathbf{v}_h, \varphi_h)\|_{\mathbf{H}(\text{div}_a, \Omega) \times \tilde{\mathbf{H}}_1^1(\Omega)}^2 \quad \forall (\mathbf{v}_h, \varphi_h) \in \mathbf{H}_h \times Z_h.$$

Remark 3.3. We recall that the constant α appearing in Lemma 3.2, depends on κ_1, κ_2 and σ , but it is independent of the viscosity. Notice also that the optimal value for the first augmentation parameter is the middle point of the relevant interval suggested by the stability analysis of Lemmas 2.1 and 3.2, *i.e.*, $\kappa_1 = 1/\sigma_{\min}$ (see *e.g.* [5], Sect. 3).

We continue with the following discrete analogue to Lemma 2.2.

Lemma 3.4. *There exists $\tilde{\beta} > 0$ independent of $\kappa_1, \kappa_2, \sigma, \nu$ and h , such that*

$$\sup_{\substack{(\mathbf{v}_h, \varphi_h) \in \mathbf{H}_h \times Z_h \\ (\mathbf{v}_h, \varphi_h) \neq 0}} \frac{|B((\mathbf{v}_h, \varphi_h), q_h)|}{\|(\mathbf{v}_h, \varphi_h)\|_{\mathbf{H}(\text{div}_a, \Omega) \times \tilde{\mathbf{H}}_1^1(\Omega)}} \geq \tilde{\beta} \|q_h\|_{L_1^2(\Omega)} \quad \forall q_h \in \mathbf{Q}_h.$$

Proof. Let $k \geq 0$ and $q_h \in \mathbf{Q}_h$. From Theorem 3.4 and Corollary 3.6 in [25], we know that there exist $\mathbf{v}_h \in \mathbf{H}_h$ and $\tilde{\beta} > 0$ such that,

$$\frac{\int_{\Omega} q_h \text{div}_a \mathbf{v}_h r \, \text{d}rdz}{\|\mathbf{v}_h\|_{\mathbf{H}(\text{div}_a, \Omega)}} \geq \tilde{\beta} \|q_h\|_{L_1^2(\Omega)}.$$

Therefore, from this inequality we can assert that

$$\begin{aligned} \sup_{\substack{(\mathbf{v}_h, \varphi_h) \in \mathbf{H}_h \times Z_h \\ (\mathbf{v}_h, \varphi_h) \neq 0}} \frac{|B((\mathbf{v}_h, \varphi_h), q_h)|}{\|(\mathbf{v}_h, \varphi_h)\|_{\mathbf{H}(\text{div}_a, \Omega) \times \tilde{\mathbf{H}}_1^1(\Omega)}} &\geq \frac{|B((\mathbf{v}_h, 0), q_h)|}{\|(\mathbf{v}_h, 0)\|_{\mathbf{H}(\text{div}_a, \Omega) \times \tilde{\mathbf{H}}_1^1(\Omega)}} \\ &= \frac{\int_{\Omega} q_h \text{div}_a \mathbf{v}_h r \, \text{d}rdz}{\|\mathbf{v}_h\|_{\mathbf{H}(\text{div}_a, \Omega)}} \\ &\geq \tilde{\beta} \|q_h\|_{L_1^2(\Omega)}. \end{aligned} \quad \square$$

We are now in a position to state the main result of this section which yields the solvability of the discrete formulation (3.4).

Theorem 3.5. *Let k be a non-negative integer and let \mathbf{H}_h, Z_h and \mathbf{Q}_h be given by (3.1)–(3.3), respectively. Then, there exists a unique solution $((\mathbf{u}_h, \omega_h), p_h) \in (\mathbf{H}_h \times Z_h) \times \mathbf{Q}_h$ to problem (3.4) and there exists a positive constant $C > 0$ such that the following continuous dependence result holds:*

$$\|((\mathbf{u}_h, \omega_h), p_h)\|_{(\mathbf{H}(\text{div}_a, \Omega) \times \tilde{\mathbf{H}}_1^1(\Omega)) \times L_1^2(\Omega)} \leq C \|\mathbf{f}\|_{L_1^2(\Omega)^2}.$$

Moreover, there exists a constant $\widehat{C} > 0$ such that

$$\begin{aligned} & \| \mathbf{u} - \mathbf{u}_h \|_{\mathbf{H}(\operatorname{div}_a, \Omega)} + \| \omega - \omega_h \|_{\widetilde{\mathbf{H}}_1^1(\Omega)} + \| p - p_h \|_{L_1^2(\Omega)} \\ & \leq \widehat{C} \left\{ \inf_{\mathbf{v}_h \in \mathbf{H}_h} \| \mathbf{u} - \mathbf{v}_h \|_{\mathbf{H}(\operatorname{div}_a, \Omega)} + \inf_{\varphi_h \in Z_h} \| \omega - \varphi_h \|_{\widetilde{\mathbf{H}}_1^1(\Omega)} + \inf_{q_h \in Q_h} \| p - q_h \|_{L_1^2(\Omega)} \right\}, \end{aligned} \tag{3.5}$$

where C and \widehat{C} are independent of ν and h , and the triplet $((\mathbf{u}, \omega), p) \in (\mathbf{H}_\diamond(\operatorname{div}_a, \Omega) \times \widetilde{\mathbf{H}}_{1,\diamond}^1(\Omega)) \times L_{1,0}^2(\Omega)$ is the unique solution to problem (2.3).

Proof. By virtue of Lemmas 3.2 and 3.4, the proof follows from a straightforward application of ([19], Thm. II.1.1). \square

3.3. Convergence analysis

According to the theorem above, it only remains to prove that \mathbf{u}, ω and p can be conveniently approximated by functions in \mathbf{H}_h, Z_h and Q_h , respectively. With this purpose, we introduce the Raviart–Thomas global interpolation operator $\mathcal{R}_h : \mathbf{H}_1^1(\Omega)^2 \rightarrow \mathbf{H}_h$ (see e.g. [25], Appendix). For this operator, we review some properties to be used in the sequel. The corresponding proofs can be found in ([25], Cor. A.6):

Lemma 3.6. *For all $\mathbf{v} \in \mathbf{H}_1^{k+1}(\Omega)^2$, with $\operatorname{div}_a \mathbf{v} \in \mathbf{H}_1^{k+1}(\Omega)$, and $(\sum_{T \in \mathcal{T}_h} |\operatorname{div}_a \mathcal{R}_h \mathbf{v}|_{\mathbf{H}_1^{k+1}(T)}^2)^{1/2} < \tilde{c}$, there exists $C > 0$, independent of h , such that*

$$\| \mathbf{v} - \mathcal{R}_h \mathbf{v} \|_{\mathbf{H}(\operatorname{div}_a, \Omega)} \leq Ch^{k+1} \left(\| \mathbf{v} \|_{\mathbf{H}_1^{k+1}(\Omega)^2} + \| \operatorname{div}_a \mathbf{v} \|_{\mathbf{H}_1^{k+1}(\Omega)} + \left(\sum_{T \in \mathcal{T}_h} |\operatorname{div}_a \mathcal{R}_h \mathbf{v}|_{\mathbf{H}_1^{k+1}(T)}^2 \right)^{1/2} \right).$$

Let \mathcal{P}_h be the orthogonal projection from $L_1^2(\Omega)$ onto the finite element subspace Q_h . We have that \mathcal{P}_h satisfies the following error estimate (see [23]):

Lemma 3.7. *There exists $C > 0$, independent of h , such that for all $q \in \mathbf{H}_1^{k+1}(\Omega)$:*

$$\| q - \mathcal{P}_h q \|_{L_1^2(\Omega)} \leq Ch^{k+1} \| q \|_{\mathbf{H}_1^{k+1}(\Omega)}.$$

On the other hand, for any φ sufficiently smooth, we are able to employ the Lagrange interpolation operator $\Pi_h : \widetilde{\mathbf{H}}_1^1(\Omega) \cap \mathbf{H}_1^2(\Omega) \rightarrow Z_h$. Moreover, there holds the following error estimate, whose proof can be found in ([41], Lem. 6.3).

Lemma 3.8. *There exists $C > 0$, independent of h , such that for all $\varphi \in \mathbf{H}_1^{k+2}(\Omega)$:*

$$\| \varphi - \Pi_h \varphi \|_{\widetilde{\mathbf{H}}_1^1(\Omega)} \leq \begin{cases} Ch^{k+1} \| \varphi \|_{\mathbf{H}_1^{k+2}(\Omega)} & \text{for } \nu \in (0, 1], \\ Ch^{k+1} \nu^{1/2} \| \varphi \|_{\mathbf{H}_1^{k+2}(\Omega)} & \text{for } \nu > 1. \end{cases}$$

We now turn to the statement of convergence properties of the discrete problem (3.4).

Theorem 3.9. *Let $k \geq 0$ and let \mathbf{H}_h, Z_h and Q_h be given by (3.1), (3.2), and (3.3), respectively. Let $((\mathbf{u}, \omega), p) \in (\mathbf{H}_\diamond(\operatorname{div}_a, \Omega) \times \widetilde{\mathbf{H}}_{1,\diamond}^1(\Omega)) \times L_{1,0}^2(\Omega)$ and $((\mathbf{u}_h, \omega_h), p_h) \in (\mathbf{H}_h \times Z_h) \times Q_h$ be the unique solutions to the continuous and discrete problems (2.3) and (3.4), respectively. Assume that $\mathbf{u} \in \mathbf{H}_1^{k+1}(\Omega)^2$, $\operatorname{div}_a \mathbf{u} \in \mathbf{H}_1^{k+1}(\Omega)$, $(\sum_{T \in \mathcal{T}_h} |\operatorname{div}_a \mathcal{R}_h \mathbf{u}|_{\mathbf{H}_1^{k+1}(T)}^2)^{1/2} < \tilde{c}$, $\omega \in \mathbf{H}_1^{k+2}(\Omega)$, and $p \in \mathbf{H}_1^{k+1}(\Omega)$. Then, the following error estimate holds true*

$$\begin{aligned} & \| \mathbf{u} - \mathbf{u}_h \|_{\mathbf{H}(\operatorname{div}_a, \Omega)} + \| \omega - \omega_h \|_{\widetilde{\mathbf{H}}_1^1(\Omega)} + \| p - p_h \|_{L_1^2(\Omega)} \\ & \leq Ch^{k+1} \left(\| \mathbf{u} \|_{\mathbf{H}_1^{k+1}(\Omega)^2} + \| \operatorname{div}_a \mathbf{u} \|_{\mathbf{H}_1^{k+1}(\Omega)} + \left(\sum_{T \in \mathcal{T}_h} |\operatorname{div}_a \mathcal{R}_h \mathbf{u}|_{\mathbf{H}_1^{k+1}(T)}^2 \right)^{1/2} + \gamma \| \omega \|_{\mathbf{H}_1^{k+2}(\Omega)} + \| p \|_{\mathbf{H}_1^{k+1}(\Omega)} \right), \end{aligned}$$

where $\gamma = 1$ for $\nu \in (0, 1]$ or $\gamma = \nu^{1/2}$ for $\nu > 1$, and where $C > 0$, is independent of ν and h .

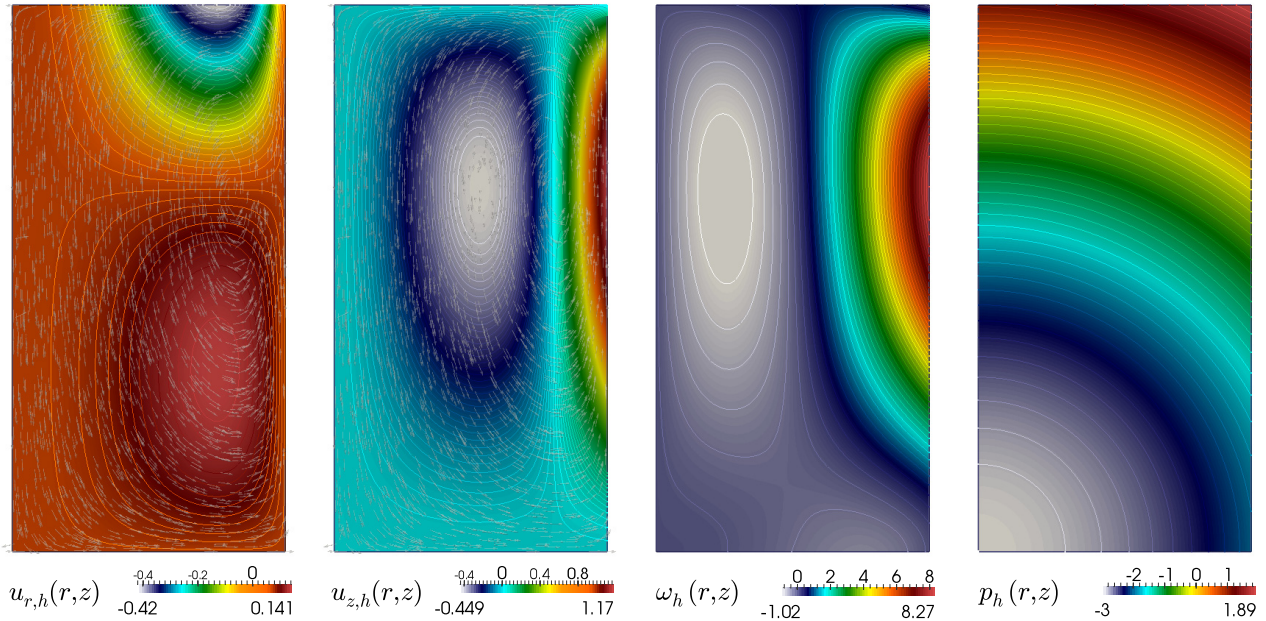


FIGURE 2. Approximate radial and longitudinal velocities, vorticity and pressure, obtained with lowest order Raviart–Thomas, piecewise linear, and piecewise constant elements, respectively. Errors with respect to the exact solutions given in (4.1) are presented in Table 1.

Proof. The proof follows from (3.5) and error estimates from Lemmas 3.6, 3.7 and 3.8. \square

Finally, we stress that our developed framework could be easily adapted to analyze other families of finite elements. For instance, considering **BDM**-based finite elements.

4. NUMERICAL TESTS

In what follows, we present four numerical examples illustrating the performance of the FE method described in Section 3, and which confirm its robustness and the previously derived theoretical error bounds.

4.1. Experimental convergence

We start by studying the accuracy of the proposed augmented formulation. This is carried out by computing errors in different norms, between the finite element approximation on successively refined non-uniform partitions \mathcal{T}_h of Ω and the following exact solution to (1.4a)–(1.4e):

$$\begin{aligned} \mathbf{u}(r, z) &= \begin{pmatrix} r^3(r-1)z(3z-4) \\ -r^2(5r-4)z^2(z-2) \end{pmatrix}, \\ \omega(r, z) &= -z^2(z-2)r(15r-8) - r^3(r-1)(6z-4), \quad p(r, z) = r^2 + z^2 - 3, \end{aligned} \quad (4.1)$$

defined on the rectangular meridional domain $\Omega = (0, 1) \times (0, 2)$, and satisfying $\mathbf{u} \cdot \mathbf{n} = 0$ on $\Gamma \cup \Gamma_s$ and $\omega = 0$ on Γ_s . In this case, we impose a non-homogeneous Dirichlet condition for the vorticity on Γ , and the model and stabilization parameters are set as $\sigma = 0.1$, $\nu = 0.01$, $\kappa_1 = 1/\sigma$, $\kappa_2 = 0.01$. The approximate solutions computed with the augmented formulation on a mesh with 263 680 triangular elements are presented in Figure 2.

TABLE 1. Experimental convergence of the augmented $\mathbf{RT}_k^a - \mathbb{P}_{k+1} - \mathbb{P}_k$ FE approximation ($k = 0$, top rows, and $k = 1$ bottom rows) of the steady axisymmetric Brinkman flow with respect to exact solutions.

d.o.f.	h	$\mathbf{e}(\mathbf{u}_h)_{\mathbf{H}(\text{div}_n, \Omega)}$	rate $_h$	$\mathbf{e}(\omega_h)_{\tilde{\mathbf{H}}_1^1(\Omega)}$	rate $_h$	$\mathbf{e}(p_h)_{L_1^2(\Omega)}$	rate $_h$
Augmented $\mathbf{RT}_0^a - \mathbb{P}_1 - \mathbb{P}_0$ finite elements							
19	1.414210	0.526498	–	0.183847	–	0.622498	–
61	0.707107	0.364212	0.957705	0.086790	1.082910	0.300851	1.049021
217	0.353553	0.191531	0.927205	0.040179	1.111072	0.157299	0.935535
817	0.176777	0.096252	0.992675	0.019496	1.043225	0.079496	0.984544
3169	0.088388	0.047973	1.004653	0.009621	1.018952	0.039855	0.996102
12481	0.044194	0.023970	1.000974	0.004774	1.010951	0.019941	0.999006
49537	0.022097	0.012116	0.984271	0.002348	1.023517	0.009972	0.999747
197377	0.011048	0.006213	0.963525	0.001127	1.058250	0.004986	0.999935
789583	0.005215	0.003351	0.985378	0.000582	1.025371	0.002491	0.999758
Augmented $\mathbf{RT}_1^a - \mathbb{P}_2 - \mathbb{P}_1$ (discontinuous) finite elements							
53	1.414210	0.689210	–	0.152660	–	0.119338	–
185	0.707107	0.204407	1.813379	0.034605	2.141251	0.039306	1.602262
689	0.353553	0.052878	1.950742	0.008639	2.001953	0.010070	1.964559
2657	0.176777	0.013985	1.918736	0.002130	2.019899	0.002543	1.985046
10433	0.088388	0.003552	1.977039	0.000475	2.162347	0.000637	1.997301
41345	0.044194	0.000888	1.998771	0.000104	2.190724	0.000159	1.995295
164609	0.022097	0.000218	2.024992	2.504e-5	2.057592	3.988e-5	2.002663
656897	0.011048	5.464e-5	1.998801	6.099e-6	2.037631	1.097e-5	1.987941
2624513	0.005524	1.353e-5	1.996387	1.502e-6	2.012571	2.593e-6	1.986785

We also compute rates of convergence from one refinement level (associated to a partition of size h) to the next one (with a mesh of size $\hat{h} < h$) as

$$\text{rate}_h = \frac{\log(\text{error}_h / \text{error}_{\hat{h}})}{\log(h / \hat{h})}.$$

These values are displayed in Table 1 for two families of finite elements $\mathbf{RT}_k^a - \mathbb{P}_{k+1} - \mathbb{P}_k$, with $k = 0$ and $k = 1$, where we observe a convergence of order h^{k+1} for all fields in the relevant norms.

4.2. Axisymmetric Brinkman flow on a settling tank

In our next example, we simulate a common scenario in wastewater treatment processes, that is a settling tank, where the accurate rendering of flow is of interest. The geometry depicted in Figure 3 (see also [4, 21]) represents a half cross-section of a cylindrical vessel with the following types of boundaries: inlet Γ_{in} , outlet Γ_{out} , symmetry axis Γ_s , overflow Γ_c , and walls (the remainder of $\partial\Omega$).

Boundary conditions assume the following configuration. On walls and symmetry axis we allow a slip velocity, that is $\mathbf{u} \cdot \mathbf{n} = 0$; normal velocities are imposed on the inlet, outlet and overflow as $q_{in} = \frac{1}{8}(\frac{4r^2}{9} - 1)$, $q_{out} = 0.01125$, $q_c = 0.00125$, respectively. Zero vorticity is imposed on the walls, symmetry axis, outlet and overflow, whereas on the inlet we set $w_{in} = \frac{r}{5}$. The external force is assumed to be zero.

An unstructured mesh of 107 882 triangles and 54 420 nodes was constructed, and we employed the following model and stabilization parameters: $\sigma = 0.1$, $\nu = 0.01$, $\kappa_1 = 1/\sigma$, $\kappa_2 = 0.01$. Radial and vertical components of the velocity, vorticity and pressure are approximated with $\mathbf{RT}_0^a - \mathbb{P}_1 - \mathbb{P}_0$ elements. The numerical results are displayed in Figure 4.

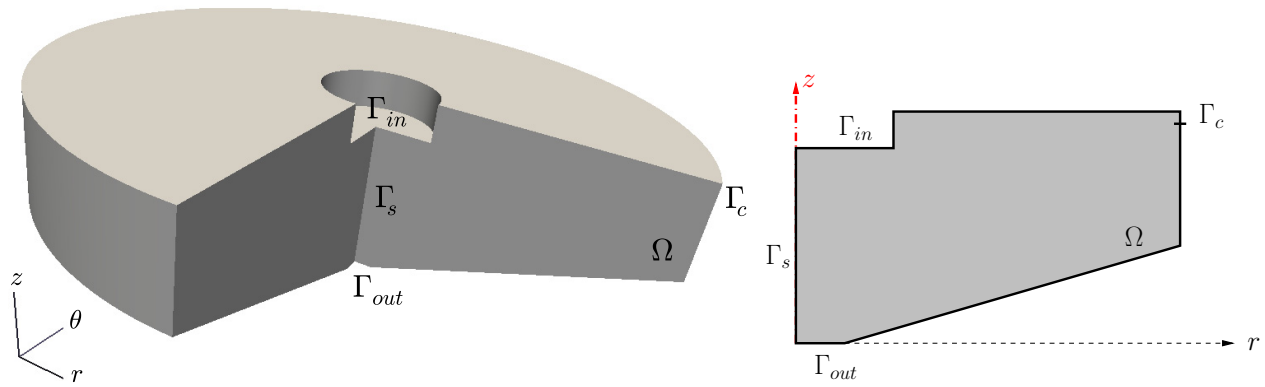


FIGURE 3. Sketch of a half cross section of a settling tank of maximum radius 8 m, total height of 5m, inlet disk of 1.5m of radius, overflow annulus of 0.5 m of edge, and outlet disk with a radius of 0.5 m.

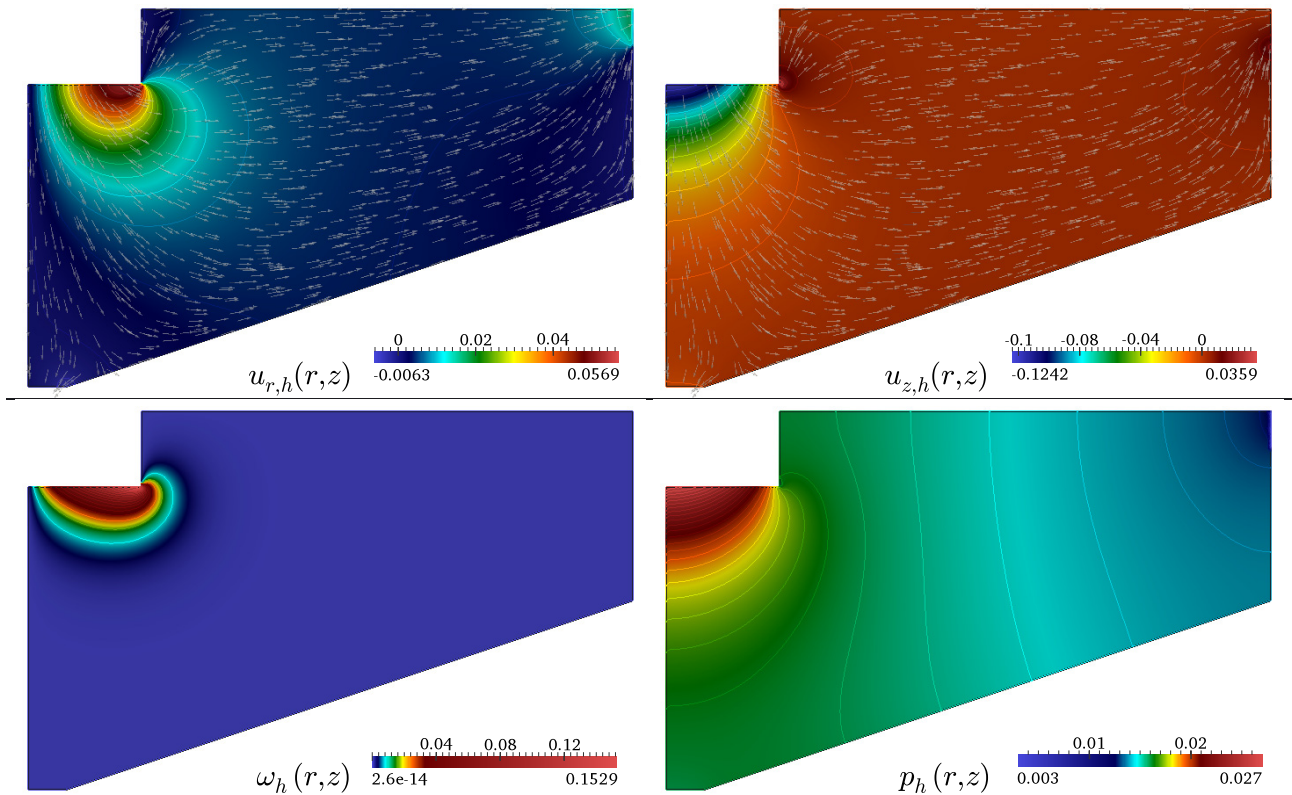


FIGURE 4. Approximate solutions of the Brinkman axisymmetric problem on a settling tank. The used mesh consists of 107 882 elements.

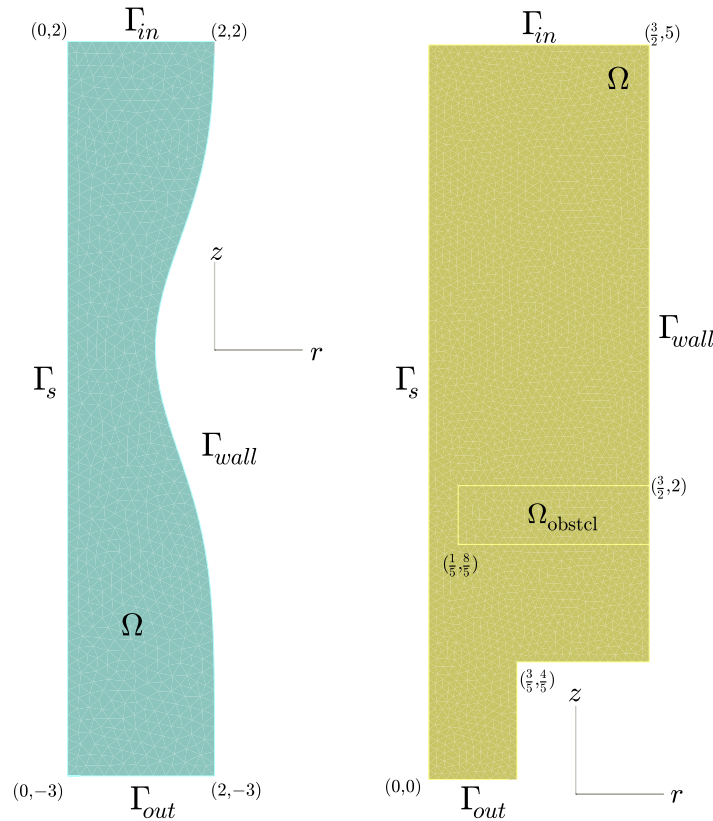


FIGURE 5. Sketch of a half cross section of an idealized artery with symmetric stenosis (left) and a cylindrical filter with sudden contraction (right).

4.3. Blood flow through an axisymmetric stenosed artery

Next, we present the simulation of a simplified model of arterial blood flow in the presence of a symmetric stenotic region on the vessel wall (see *e.g.* [42,47]). We are only interested in the laminar regime, so (1.4a)–(1.4c) (with a simple Newtonian model for the blood) will suffice to describe the main components of the flow. The computational domain consists on a half cross-section of a vessel segment of length 5 cm and maximum radius 1cm (see a sketch in Fig. 5, left). The boundaries are the inlet Γ_{in} ($z = 2, r \in [0, 1]$) outlet Γ_{out} ($z = -3, r \in [0, 1]$), symmetry axis Γ_s ($z \in [-3, 2], r = 0$), and arterial wall ($z \in [-3, 2], r = 1 + \delta \exp(-sz^2)(z+3)(z+2)/6$), with $\delta = 0.4$ and $s = 0.8$. Boundary data are set in the following manner: on Γ_{in} we impose a Poiseuille flow of maximum normal velocity with norm $Re = 1/\nu$, and a consistent vorticity $w = 2r/\nu$. On symmetry axis and arterial wall we set zero normal velocity and vorticity, whereas on the outlet we use $\mathbf{u} \cdot \mathbf{t} = 0$ and $p = 0$. The conditions on Γ_{out} were not covered in our analysis, but we stress that they can be also treated following *e.g.* [4,5]. The flow regime is characterized by the parameters $\nu = 0.01$, and we set $\sigma = 0.01, \kappa_1 = 1/\sigma, \kappa_2 = 0.1$. An unstructured mesh of 43 712 elements and 21 857 nodes was built to discretize the axisymmetric domain Ω . Figure 6 displays approximate solutions using $\mathbf{RT}_0^a - \mathbb{P}_1 - \mathbb{P}_0$ approximations for velocity, vorticity and pressure. The narrowing of the vessel at the stenosis yields flow resistance and a rapid pressure drop. For visualization purposes, we also depict a rotational extrusion of 290 degrees of these solutions in Figure 8.

In order to assess the robustness of the method with respect to the fluid viscosity, we have also run the same test taking now $\sigma = 1$ and considering decreasing values of viscosity, from $\nu = 100$ down to $\nu = 1e-30$, the latter

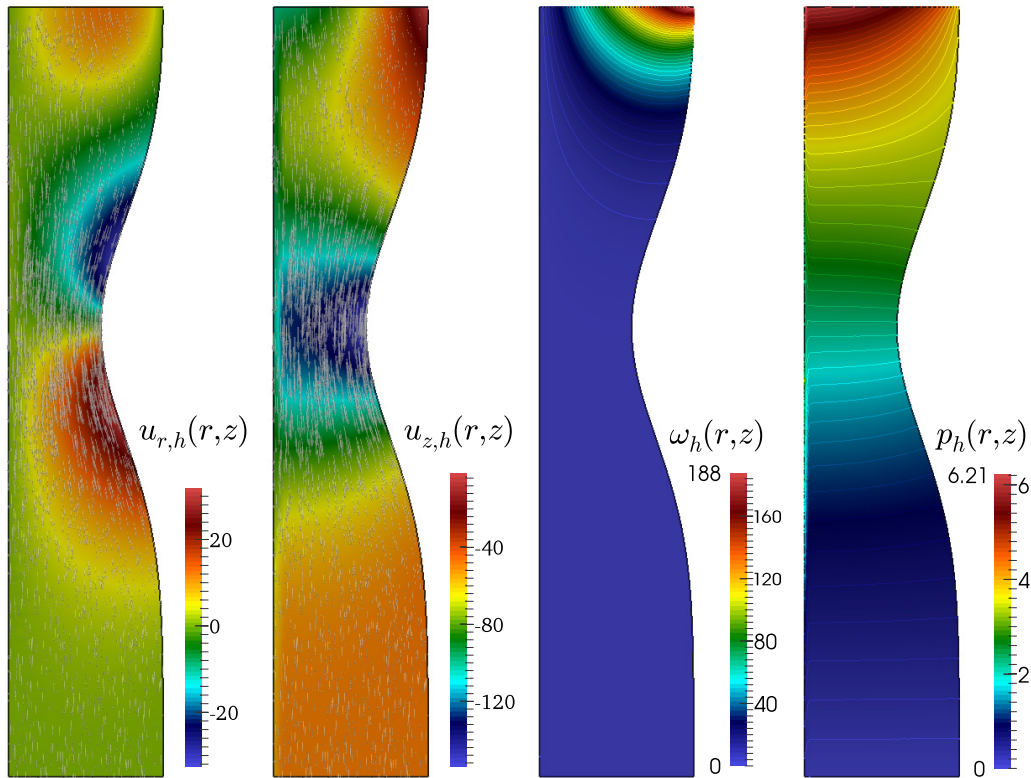


FIGURE 6. Augmented mixed finite element approximation of the Brinkman axisymmetric problem on a stenosed artery (from left to right: radial velocity, vertical velocity, vorticity and pressure). Solutions on the half cross-section discretized with 43 712 triangular elements.

TABLE 2. Norm of the velocity and vorticity fields over the axisymmetric domain representing a stenosed artery, for different values of the viscosity coefficient.

ν	100	10	1	0.1	0.01	0.001	1.0e-04	1.0e-05	1.0e-10	1.0e-20	1.0e-30
$\ \mathbf{u}_h\ _{\mathbf{H}(\text{div}_a, \Omega)}$	113.179	100.015	98.6043	98.6043	98.4491	98.4478	98.4477	98.4477	98.4477	98.4477	98.4477
$\ \omega_h\ _{\bar{\mathbf{H}}^1(\Omega)}$	1421.23	451.291	148.461	62.2763	45.4105	43.3643	43.1546	43.1336	43.1313	43.1313	43.1313

corresponding to the pure Darcy limit. The maximal normal Poiseuille velocity and vorticity profiles are fixed to 100 and $200r$, respectively. Stabilization parameters are now $\kappa_1 = 1$ and $\kappa_2 = 0.1$. In all computations the solution remains stable, as evidenced from Table 2, where we display the velocity and vorticity norms for different values of ν , and also from Figure 7, which portrays the field variables over the line $r = 0.1$, corresponding to an annular section on the extruded domain. For viscosities smaller than $1e-5$, the profiles practically coincide.

4.4. Flow in a contracting cylinder containing a porous obstacle

We close this section with a simulation relevant in the modeling of oil filters. We consider a cylindrical domain with an annular porous obstacle, whose half cross-section is depicted in the right panel of Figure 5, and assume that the permeability inside the obstacle Ω_{obstcl} is much lower than that of the rest of the domain.

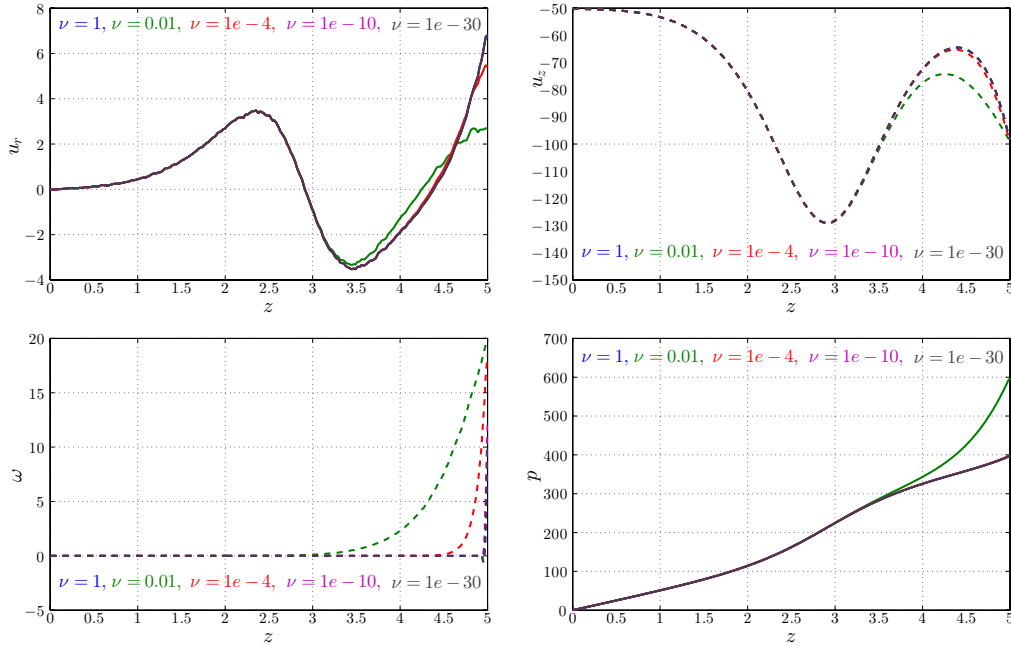


FIGURE 7. Approximation of radial and vertical velocity components (top left and right, respectively), vorticity and pressure fields (bottom row, left and right) computed over the midline $r = 0.1$ for different values of the viscosity coefficient.

This assumption is accounted for by setting

$$\sigma = \sigma(r, z) = \begin{cases} \sigma_{\max} = 100 & \text{in } \Omega_{\text{obstcl}}, \\ \sigma_{\min} = 0.001 & \text{otherwise.} \end{cases}$$

As in the previous test case, we here impose the Poiseuille normal velocity inflow $\mathbf{u} \cdot \mathbf{n} = 2/75r(r - 3/2)$ and the compatible vorticity $\omega = 2/75(r - 3/2)$ on Γ_{in} , on Γ_s and Γ_{wall} we set zero normal velocity and vorticity, and on the outlet we do not constraint flow nor pressure. Other model parameters are chosen as $\nu = 0.01$, $\kappa_1 = 1/\sigma_{\min}$, $\kappa_2 = 0.1$, and $\mathbf{f} = \mathbf{0}$. The axisymmetric domain was discretized with an unstructured mesh of 122303 triangular elements and 61021 vertices.

The approximate solutions obtained with the proposed augmented $\mathbf{RT}_0^a - \mathbb{P}_1 - \mathbb{P}_0$ method are displayed in Figure 9. As expected (see a similar study for the Cartesian case in [5]), we can observe velocity patterns avoiding the annular porous obstacle and concentrating on the symmetry axis, and pressure profiles with high gradients near the obstacle boundary.

5. CONCLUSIONS

In this work, we have presented a new stabilized mixed finite element method for the discretization of a vorticity-velocity-pressure formulation of the Brinkman problem in axisymmetric coordinates. A rigorous solvability analysis of both continuous and discrete problems was carried out using tools from the Babuška–Brezzi theory, and we derived optimal convergence rates (and robust with respect to viscosity) in the natural norms for the particular case of Raviart–Thomas approximations of order k for velocities, and piecewise polynomials of degrees $k + 1$ and k approximating the scalar vorticity and pressure, respectively, for $k \geq 0$. We provided a few numerical tests confirming our theoretical findings regarding optimal convergence of the approximate

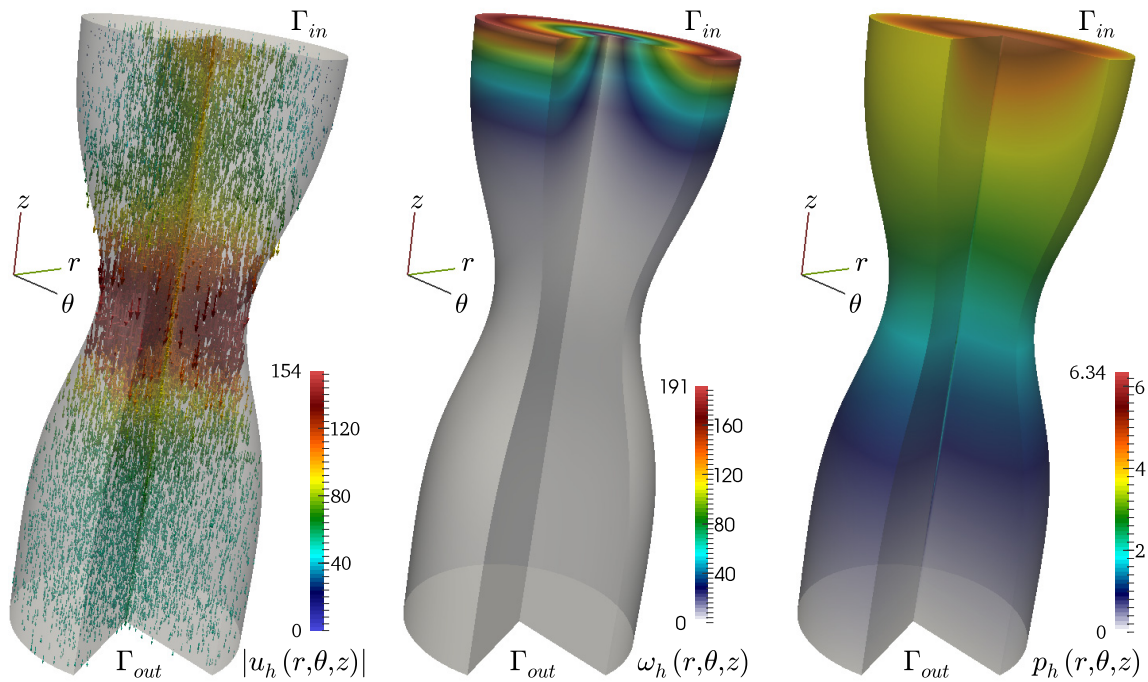


FIGURE 8. Augmented mixed finite element approximation of the Brinkman axisymmetric problem on a stenosed artery (from left to right: velocity, vorticity and pressure). Rotational extrusion of 290 degrees to the three-dimensional domain.

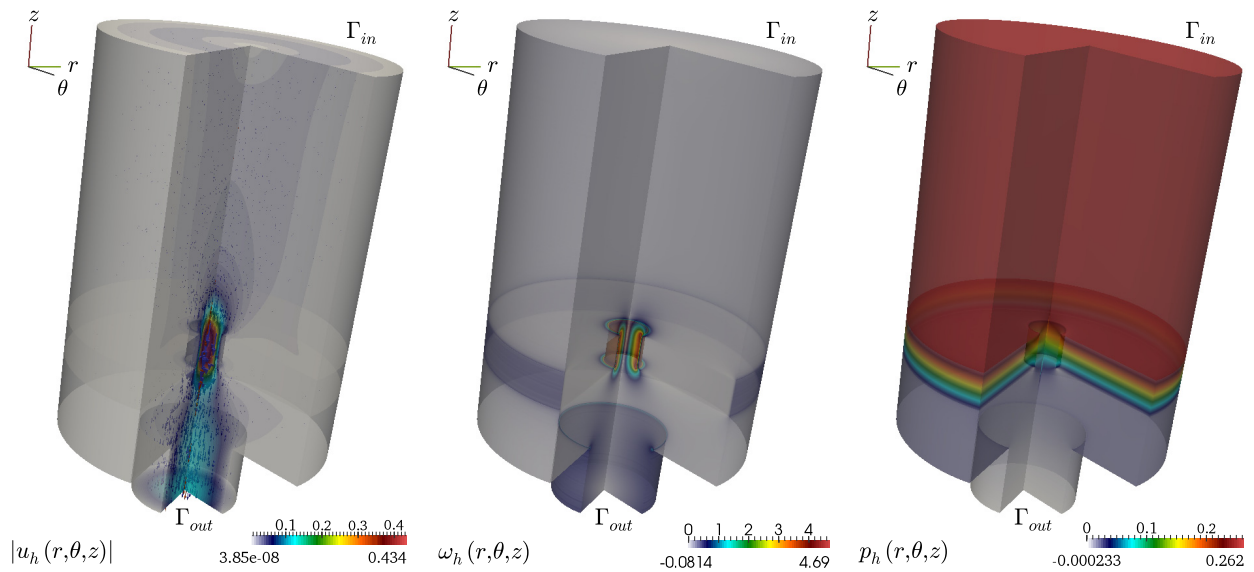


FIGURE 9. Augmented mixed finite element approximation of the Brinkman axisymmetric problem on an idealized oil filter. Rotational extrusion of velocity, vorticity, and pressure (left, center, and right, respectively) to the full three-dimensional domain.

solutions and showing that our framework can be successfully applied in a wide range of interesting applications as wastewater treatment processes, the simulation of arterial blood flow, and the modeling of oil filters. Possible extensions of this work include the study of vorticity-based formulations of axisymmetric time-dependent Navier–Stokes equations, the incorporation of a larger class of boundary conditions, and the use of the developed theory in the coupling of flow equations and nonlinear transport problems.

Acknowledgements. We gratefully acknowledge the suggestions made by the referees, which have significantly improved the presentation of this paper.

REFERENCES

- [1] N. Abdellatif and C. Bernardi, A new formulation of the Stokes problem in a cylinder, and its spectral discretization. *ESAIM: M2AN* **38** (2004) 781–810.
- [2] N. Abdellatif, N. Chorfi and S. Trabelsi, Spectral discretization of the axisymmetric vorticity, velocity and pressure formulation of the Stokes problem. *J. Sci. Comput.* **47** (2011) 419–440.
- [3] M. Amara, D. Capatina-Papaghiuc, B. Denel and P. Terpolilli, Mixed finite element approximation for a coupled petroleum reservoir model. *ESAIM: M2AN* **39** (2005) 349–376.
- [4] V. Anaya, D. Mora and R. Ruiz-Baier, An augmented mixed finite element method for the vorticity-velocity-pressure formulation of the Stokes equations. *Comput. Methods Appl. Mech. Engrg.* **267** (2013) 261–274.
- [5] V. Anaya, D. Mora, G.N. Gatica and R. Ruiz-Baier, An augmented velocity-vorticity-pressure formulation for the Brinkman problem. To appear in *Int. J. Numer. Methods Fluids* (2015).
- [6] V. Anaya, D. Mora, R. Oyarzúa and R. Ruiz-Baier, *A priori* and *a posteriori* error analysis for a vorticity-based mixed formulation of the generalized Stokes equations. CI²MA preprint 2014-20. Available from <http://www.ci2ma.udec.cl/publicaciones/prepublicaciones>.
- [7] S.M. Aouadi, C. Bernardi and J. Satouri, Mortar spectral element discretization of the Stokes problem in axisymmetric domains. *Numer. Methods Partial Differ. Eq.* **30** (2014) 44–73.
- [8] F. Assous, P. Ciarlet and S. Labrunie, Theoretical tools to solve the axisymmetric Maxwell equations. *Math. Methods Appl. Sci.* **25** (2002) 49–78.
- [9] F. Assous, P. Ciarlet, S. Labrunie and J. Segré, Numerical solution to the time-dependent Maxwell equations in axisymmetric singular domains: the singular complement method. *J. Comput. Phys.* **191** (2003) 147–176.
- [10] M. Azaiez, A spectral element projection scheme for incompressible flow with application to the unsteady axisymmetric Stokes problem. *J. Sci. Comput.* **17** (2002) 573–584.
- [11] G.R. Barrenechea and F. Valentin, An unusual stabilized finite element method for a generalized Stokes problem. *Numer. Math.* **92** (2002) 653–677.
- [12] T. Barrios, R. Bustinza, G. García and E. Hernández, On stabilized mixed methods for generalized Stokes problem based on the velocity-pseudostress formulation: a priori error estimates. *Comput. Methods Appl. Mech. Engrg.* **237/240** (2012) 78–87.
- [13] Z. Belhachmi, C. Bernardi and S. Deparis, Weighted Clément operator and application to the finite element discretization of the axisymmetric Stokes problem. *Numer. Math.* **105** (2002) 217–247.
- [14] Z. Belhachmi, C. Bernardi, S. Deparis and F. Hecht, An efficient discretization of the Navier-Stokes equations in an axisymmetric domain. Part 1: The discrete problem and its numerical analysis. *J. Sci. Comput.* **27** (2006) 97–110.
- [15] A. Bermúdez, C. Reales, R. Rodríguez and P. Salgado, Numerical analysis of a finite element method for the axisymmetric eddy current model of an induction furnace. *IMA J. Numer. Anal.* **30** (2010) 654–676.
- [16] A. Bermúdez, C. Reales, R. Rodríguez and P. Salgado, Mathematical and numerical analysis of a transient eddy current axisymmetric problem involving velocity terms. *Numer. Methods Partial Differ. Eq.* **28** (2012) 984–1012.
- [17] C. Bernardi and N. Chorfi, Spectral discretization of the vorticity, velocity, and pressure formulation of the Stokes problem. *SIAM J. Numer. Anal.* **44** (2007) 826–850.
- [18] C. Bernardi, M. Dauge and Y. Maday, *Spectral Methods for Axisymmetric Domains*. Gauthier-Villars, Éditions Scientifiques et Médicales Elsevier, Paris (1999).
- [19] F. Brezzi and M. Fortin, *Mixed and Hybrid Finite Element Methods*. Springer Verlag, New York (1991).
- [20] R. Bürger, S. Kumar and R. Ruiz-Baier, Discontinuous finite volume element approximation for a fully coupled Stokes flow-transport problem. CI²MA preprint 2014-25. Available from <http://www.ci2ma.udec.cl/publicaciones/prepublicaciones>.
- [21] R. Bürger, R. Ruiz-Baier and H. Torres, A stabilized finite volume element formulation for sedimentation–consolidation processes. *SIAM J. Sci. Comput.* **34** (2012) B265–B289.
- [22] J.H. Carneiro de Araujo and V. Ruas, A stable finite element method for the axisymmetric three-field Stokes system. *Comput. Methods Appl. Mech. Engrg.* **164** (1998) 267–286.
- [23] P. Clément, Approximation by finite element functions using local regularisation. *RAIRO Modél. Math. Anal. Numér.* **9** (1975) 77–84.
- [24] D.M. Copeland, J. Gopalakrishnan and M. Oh, Multigrid in a weighted space arising from axisymmetric electromagnetics. *Math. Comput.* **79** (2010) 2033–2058.

- [25] V.J. Ervin, Approximation of axisymmetric Darcy flow using mixed finite element methods. *SIAM J. Numer. Anal.* **51** (2013) 1421–1442.
- [26] V.J. Ervin, Approximation of coupled Stokes–Darcy flow in an axisymmetric domain. *Comput. Methods Appl. Mech. Engrg.* **258** (2013) 96–108.
- [27] G.N. Gatica, A Simple Introduction to the Mixed Finite Element Method. Theory and Applications. *Springer Briefs in Mathematics*. Springer, Cham, Heidelberg, New York, Dordrecht London (2014).
- [28] G.N. Gatica, A. Márquez, R. Oyarzúa and R. Rebolledo, Analysis of an augmented fully-mixed approach for the coupling of quasi-Newtonian fluids and porous media. *Comput. Methods Appl. Mech. Engrg.* **270** (2014) 76–112.
- [29] G.N. Gatica, L.F. Gatica and A. Márquez, Analysis of a pseudostress-based mixed finite element method for the Brinkman model of porous media flow. *Numer. Math.* **126** (2014) 635–677.
- [30] J. Gopalakrishnan and M. Oh, Commuting smoothed projectors in weighted norms with an application to axisymmetric Maxwell equations. *J. Sci. Comput.* **51** (2012) 394–420.
- [31] J. Gopalakrishnan and J. Pasciak, The convergence of V-cycle multigrid algorithms for axisymmetric Laplace and Maxwell equations. *Math. Comput.* **75** (2006) 1697–1719.
- [32] R. Grauer and T.C. Sideris, Numerical computation of 3D incompressible ideal fluids with swirl. *Phys. Rev. Lett.* **67** (1991) 3511–3514.
- [33] A. Guardone and L. Vigevano, Finite element/volume solution to axisymmetric conservation laws. *J. Comput. Phys.* **224** (2007) 489–518.
- [34] J. Könnö and R. Stenberg, Numerical computations with $H(\text{div})$ –finite elements for the Brinkman problem. *Comput. Geosci.* **16** (2012) 139–158.
- [35] A. Kufner, Weighted Sobolev Spaces. Wiley, New York (1983).
- [36] P. Lacoste, Solution of Maxwell equation in axisymmetric geometry by Fourier series decomposition and by use of $H(\text{rot})$ conforming finite element. *Numer. Math.* **84** (2000) 577–609.
- [37] Y.-J. Lee and H. Li, Axisymmetric Stokes equations in polygonal domains: Regularity and finite element approximations. *Comput. Math. Appl.* **64** (2012) 3500–3521.
- [38] Y.-J. Lee and H. Li, On stability, accuracy, and fast solvers for finite element approximations of the axisymmetric Stokes problem by Hood–Taylor elements. *SIAM J. Numer. Anal.* **49** (2011) 668–691.
- [39] J.-G. Liu and W.-C. Wang, Convergence analysis of the energy and helicity preserving scheme for axisymmetric flows. *SIAM J. Numer. Anal.* **44** (2006) 2456–2480.
- [40] K.A. Mardal, X.-C. Tai and R. Winther, A robust finite element method for Darcy–Stokes flow. *SIAM J. Numer. Anal.* **40** (2002) 1605–1631.
- [41] B. Mercier and G. Raugel, Resolution d’un problème aux limites dans un ouvert axisymétrique par éléments finis en r , z et séries de Fourier en θ . *RAIRO Anal. Numér.* **16** (1982) 405–461.
- [42] G. Pontrelli, Blood flow through an axisymmetric stenosis. *Proc. Int. Mech. Engrs.* **215** (2001) H01–H10.
- [43] K.R. Rajagopal, On a hierarchy of approximate models for flows of incompressible fluids through porous solids. *Math. Models Methods Appl. Sci.* **17** (2007) 215–252.
- [44] A. Riaz, M. Hesse and H.A. Tchelepi, Onset of convection in gravitationally unstable diffusive boundary layer in porous media. *J. Fluid Mech.* **548** (2006) 87–111.
- [45] V. Ruas, Mixed finite element methods with discontinuous pressures for the axisymmetric Stokes problem. *ZAMM Z. Angew. Math. Mech.* **83** (2003) 249–264.
- [46] C.G. Speziale, On the advantages of the vorticity-velocity formulations of the equations of fluid dynamics. *J. Comput. Phys.* **73** (1987) 476–480.
- [47] P.N. Tandon and U.V.S. Rana, A new model for blood flow through an artery with axisymmetric stenosis. *Int. J. Biomed. Comput.* **38** (1995) 257–267.
- [48] P. Vassilevski and U. Villa, A mixed formulation for the Brinkman problem. *SIAM J. Numer. Anal.* **52** (2014) 258–281.